Available online at www.sciencedirect.com
SCIENCE DIRECT
Journal of Catalysis 242 (2006) 110–117
JOURNAL OF CATALYSIS
www.elsevier.com/locate/jcat

Immobilization of iron porphyrins in tubular kaolinite obtained by an intercalation/delamination procedure

Shirley Nakagaki [a,*], Guilherme Sippel Machado [a], Matilte Halma [a], Antonio Augusto dos Santos Marangon [b], Kelly Aparecida Dias de Freitas Castro [a], Ney Mattoso [c], Fernando Wypych [b]

[a] *Universidade Federal do Paraná, Departamento de Química, Laboratório de Bioinorgânica e Catálise, CP 19081, CEP 81531990, Curitiba, Paraná, Brazil*
[b] *Centro de Pesquisa em Química Aplicada (CEPESQ), CP 19081, CEP 81531990, Curitiba, Paraná, Brazil*
[c] *Departamento de Física, CP 19081, CEP 81531990, Curitiba, Paraná, Brazil*

Received 19 April 2006; revised 2 June 2006; accepted 5 June 2006

Available online 3 July 2006

Abstract

This paper describes the synthesis of a first-generation iron porphyrin catalyst immobilized in a tubular/delaminated kaolinite. Kaolinite was mechanochemically intercalated with urea followed by *n*-hexylamine, and the catalyst was prepared by submitting the kaolinite/hexylamine intercalation compound to a sonication procedure in the presence of two different iron porphyrin solutions. The materials thus obtained were characterized by UV–vis and IR spectroscopies, XRD, and TEM. The procedure delaminated part of the kaolinite, yielding scroll-like nanotubes, with the metalloporphyrins immobilized in the mixture. The catalytic activity of the materials for cyclohexane and *n*-heptane oxidation was investigated using iodosylbenzene as the oxygen donor and the products were analyzed by gas chromatography. The results show a promising catalytic system for selective oxidation reactions.

Keywords: Iron porphyrin; Kaolinite; Supported catalyst; Catalysis; Oxidation; Heptane

1. Introduction

Selective catalytic oxidation of hydrocarbons by metalloporphyrins using different oxygen atom donors is one of the most attractive transformations in organic synthesis [1–3]. Synthetic metalloporphyrins, mainly iron(III) and manganese(III) complexes, have been identified as effective catalysts for a wide range of selective oxidations, mimicking cytochrome P-450 monooxygenases [4,5]. In recent years, several generations of metalloporphyrins have been prepared [2–7].

Even though very efficient homogeneous systems have been found for hydrocarbon hydroxylation and epoxidation, such problems as oxidative catalyst degradation in the presence of inert substrates are challenges that must be overcome if large-scale utilization is desired. One approach to reducing metalloporphyrin degradation is immobilization/encapsulation in different materials [6–9], which also provides site isolation of the metal center, thus minimizing catalyst self-destruction and dimerization of unhindered metalloporphyrins.

The major advantages of encapsulated catalysts are control of the reaction medium and conditions, prevention of chemical degradation, cost-effective catalyst recycling, and enhanced stability [8,9]. Selective catalytic materials may result from controlled formation of either the pore structure of the material or the solid three-dimensional network [10]. In fact, morphological control of particles is one of the major challenges associated with the industrial use of silica.

Based on the "unusual" structures and properties, layered materials, fibers, and open nanotubes are promising materials for the immobilization/encapsulation of active catalysts, which need to be transformed from homogeneous to heterogeneous

* Corresponding author. Fax: +55 41 33613186.
E-mail address: shirley@quimica.ufpr.br (S. Nakagaki).

0021-9517/$ – see front matter
doi:10.1016/j.jcat.2006.06.003

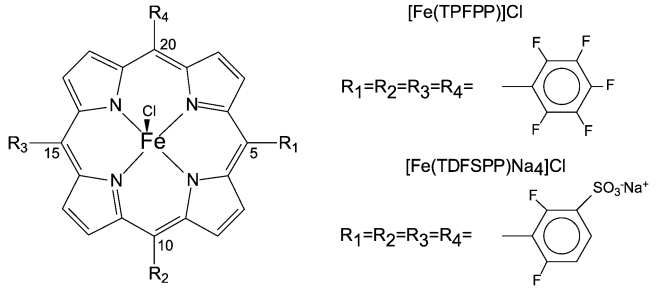

Fig. 1. Structure of the iron porphyrins used in this study: [Fe(TPFPP)]Cl = [5,10,15,20-tetrakis (pentafluorphenyl) porphyrinate iron(III)] chloride; [Fe(TDFSPP)Na_4]Cl = [tetrasodium-5,10,15,20-tetrakis (2,6-difluorphenyl-3-sulfonatophenyl) porphyrinate iron(III)] chloride.

catalysis while retaining selectivity and high activity. A typical example of layered structures, kaolinite or $Al_2Si_2O_5(OH)_4$, is a dioctahedral aluminosilicate of the 1:1 type with two distinct interlayer surfaces. One side of the layer is gibbsite-like with aluminum atoms octahedrally coordinated to corner oxygen atoms and hydroxyl groups. The other side of the layer constitutes a silica-like structure in which the silicon atoms are tetrahedrally coordinated to oxygen atoms. The adjacent layers are linked by hydrogen bonds involving aluminol (Al–OH) and siloxane (Si–O) groups. These binding forces hinder the intercalation processes, but the hydroxyl groups on the aluminum side of the layer are passive to solvation and covalent grafting reactions [11–13]. In the case of large molecules, only the surface would be expected to be grafted. In this sense, a delamination process would be helpful for providing a small number of stacked layers, producing crystals with large basal surface area [14]. Mechanochemical intercalation of urea and treatment with water under ultrasonic stirring is a very easy way to promote the delamination of kaolinite and produce high-basal area surface crystals, ideal for the grafting reaction and subsequent immobilization of metalloporphyrins.

Although kaolinite has a neutral structure and belongs to the same category of clay minerals, no report has been found so far of its use as support for the immobilization of molecules with catalytic activity. Recently, our research groups reported the immobilization of the anionic iron(III) porphyrin Na_4[Fe(TDFSPP)Cl] in silanized kaolinite and its use as a catalyst for oxidation reactions [15]. Fig. 1 shows the structure of the metalloporphyrins studied here.

Recently, it was observed that after intercalation and grafting of kaolinite, single layers or even small stacks of layers can curl, producing the so-called "halloysite-like" morphology [16], tubular or scroll-like kaolinite. The curled tubes have a silica-like surface and an inner surface with the gibbsite-like structure. As in the grafted kaolinite, the average inner diameter of the tubes is close to 250 Å [16,17], then the kaolinite nanotubes and layers can interact with the porphyrin.

The purpose of the present work was to try to develop a simple method for preparing an efficient and selective heterogeneous catalyst consisting of iron porphyrin immobilized in delaminated/curled kaolinite.

2. Experimental

2.1. Reagents

All chemicals used in this study were purchased from Aldrich, Sigma, or Merck and were of analytical grade. Iodosylbenzene (PhIO) was synthesized by hydrolysis of iodosylbenzenediacetate [18]. The solid was carefully dried under reduced pressure and kept at 5 °C. The purity was periodically controlled by iodometric titration [19].

2.2. Porphyrins

Free base porphyrin $Na_4[H_2$(TDFSPP)] and the resulting iron porphyrin complex were synthesized, purified, and characterized as described previously [20–22]. The iron complex was obtained also as described previously [15]. The iron porphyrin Fe(TPFPP)Cl was purchased from Aldrich and previously purified by a silica column.

2.3. Heterogeneous catalysts preparation

Kaolinite, previously intercalated with urea and characterized by X-ray diffraction and IR spectroscopy, was used. The solid (2 g) was magnetically stirred with methanol (50 mL) for 24 h and centrifuged, and then the supernatant was discarded. This process was repeated six more times with methanol and then repeated twice more with water (50 mL) for 2 h to intercalate water between the kaolinite layers. The solid was characterized by XRD while still moist and after 2 days of drying under air. The moist solid was magnetically stirred with *n*-hexylamine (10 mL) for 24 h twice, the suspension was centrifuged, and the supernatant was discarded. The solid (**KUH**) was characterized by XRD while still moist, after 2 h of drying under air, and after 2 days of the same air-drying process.

Kaolinite intercalated with *n*-hexylamine (**KUH**), still moist (100 mg), was suspended in 50 mL of toluene and submitted to an delamination process in an ultrasonic bath for 2 h in the presence of the catalyst, an iron porphyrin Fe(TPFPP) (2.0×10^{-3} mmol) toluene solution, resulting in an orange-colored suspension. The suspension was centrifuged, and the solid (yellow color) was washed with toluene five times. The supernatant was kept for later determination of the non-immobilized iron porphyrin by UV–vis spectroscopy. The solid was characterized by XRD and IR spectroscopy (**KUH-FP-1**).

The same procedure was repeated to obtain the solid intercalated with the anionic-charged iron porphyrin Fe(TDFSPP). An aqueous iron porphyrin solution (1.6×10^{-3} mmol) was used for this purpose. After the immobilization process, the supernatant was colorless and clear, suggesting by naked-eye inspection that all of the iron porphyrin content was immobilized in the solid **KUH** used, producing a green solid (**KUH-FP-2**).

The solid was characterized by XRD, IR spectroscopy, and transmission electronic microscopy (TEM). After use, all reagents were discarded in an appropriate container for later treatment for reuse or for final disposal.

2.4. Oxidation of cyclohexane and n-heptane by iodosylbenzene (PhIO)

Catalytic oxidation reactions were carried out in a 2-mL thermostatic glass reactor equipped with a magnetic stirrer. In a typical heterogeneous catalysis reaction, the catalyst compound (**KUH-FP-1** or **KUH-FP-2**) and iodosylbenzene was suspended in 0.300 mL of solvent (dichloromethane:acetonitrile, 1:1, V/V), and the substrate (either cyclohexane or *n*-heptane) was added, resulting in a constant compound:oxidant:substrate molar ratio of 1:20:2000. The oxidation reaction was carried out during a controlled time interval (1 h) under magnetic stirring. Sodium sulfite was added to eliminate the excess iodosylbenzene. The reaction products in solution were separated from the solid by centrifugation, and the solid catalyst was washed with dichloromethane and acetonitrile solvents. All of the extracted solution and supernatant were transferred to a volumetric flask and analyzed by gas chromatography. Product yields were determined based on PhIO with the internal standard method. The same procedure was followed in the control reactions using (a) only the substrate, (b) substrate + PhIO, and (c) substrate + PhIO + **KUH**. The procedure for homogeneous catalysis reactions was similar to that used for the heterogeneous catalysis reaction.

2.5. Techniques used

For the XRD measurements, self-oriented films were placed on neutral glass sample holders. The measurements were performed in reflection mode using a Shimadzu XRD-6000 diffractometer operating at 40 kV and 40 mA (Cu$K\alpha$ radiation $\lambda = 1.5418$ Å) with a dwell time of 1°/min.

FTIR spectra were recorded on a Biorad 3500 GX spectrophotometer in the range of 400–4000 cm^{-1}, using KBr pellets. KBr was crushed with a small amount of the solids, and the spectra were collected with a resolution of 4 cm^{-1} and accumulation of 32 scans.

UV–vis spectra were recorded in the 200–800 nm range in an HP 8452A Diode Array Spectrophotometer. All analyses were obtained with a 1-cm path length cell.

TEM was performed in a JEOL-JEM 1200–100 kV system. A drop of powder suspension of the samples was deposited on a copper grid, and the transmission electron micrographs were recorded.

Products from catalytic oxidation reactions were identified using a Shimadzu CG-14B gas chromatograph (with a flame ionization detector) with a DB-WAX capillary column (J&W Scientific).

3. Results and discussion

Fig. 2 shows the FTIR spectra of raw kaolinite (Fig. 2a) and urea-intercalated kaolinite (Fig. 2b); hydrated kaolinite produced by washing with water (Fig. 2c); and kaolinite intercalated with *n*-hexylamine (Fig. 2d). Raw kaolinite presented the typical highly ordered kaolinite, identified by the characteristic hydroxide group bands positioned at 3695, 3669, 3652, and 3620 cm^{-1}. After intercalation with urea, two new bands appeared in the OH region (3503 and 3388 cm^{-1}), attributed to interactions of the hydroxyl groups with urea, and the characteristic multiple bands in the region of 1650 cm^{-1}, attributed to internal kaolinite hydroxyl groups [23,24]. After washing the phase intercalated with urea, a typical spectrum of hydrated kaolinite was obtained with the fingerprint band positioned at 3600 and 3540 cm^{-1}. In addition, the bands attributed to urea were absent in hydrated kaolinite. The same behavior was observed after washing **KUH**, where a typical FTIR spectrum was observed, with several new bands at 3552, 3484, 3415, and 3239 cm^{-1}, attributed to the interaction of water and hexylamine molecules with the hydroxide groups of kaolinite. The FTIR spectra of **KUH-FP-1** and **KUH-FP-2** were very similar to the spectra of hydrated kaolinite (not shown).

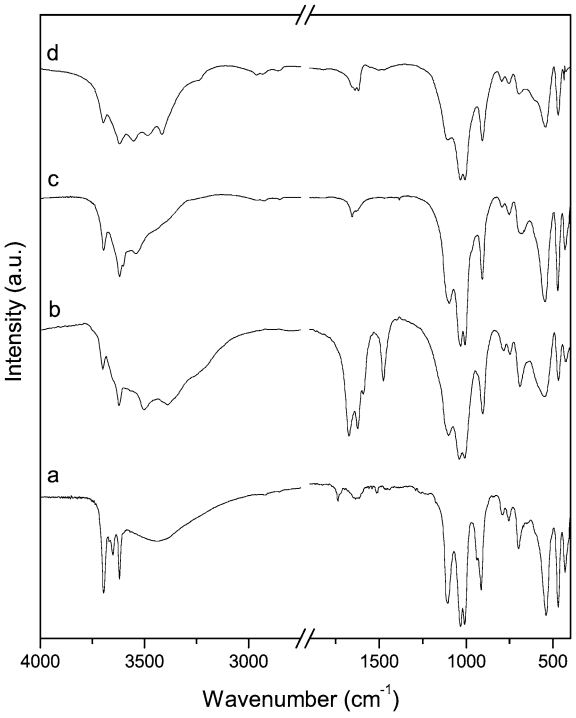

Fig. 2. FTIR spectra of raw kaolinite (a), urea intercalated kaolinite (b), hydrated kaolinite (c) and **KUH** (d), both after drying under air.

Fig. 3 shows the powder XRD patterns of raw kaolinite (Fig. 3a), kaolinite intercalated with urea (Fig. 3b), kaolinite intercalated with water and still moist (Fig. 3c), **KUH** while still moist (Fig. 3d), **KUH-FP-1** (Fig. 3e), and **KUH-FP-2** (Fig. 3f). Raw kaolinite presented the characteristic 7.1 Å basal diffraction peak, which, after intercalation with urea, migrated to the basal distance of 10.69 Å. This distance is close to the value reported in the literature of 10.76 Å [14,17]. After the urea-intercalated kaolinite was washed with water and measured in slurry, a diffraction peak was observed near 9° (2θ), attributed to fully hydrated kaolinite with a basal distance of 9.8 Å. After the hydrated kaolinite was dried under air for some hours, the basal distance collapsed to 8.4 Å, attributed to the keying of water molecules into the kaolinite layer [17].

KUH that was still moist exhibited an intense peak near 3° (2θ) with a basal distance of 26.16 Å, attributed to the in-

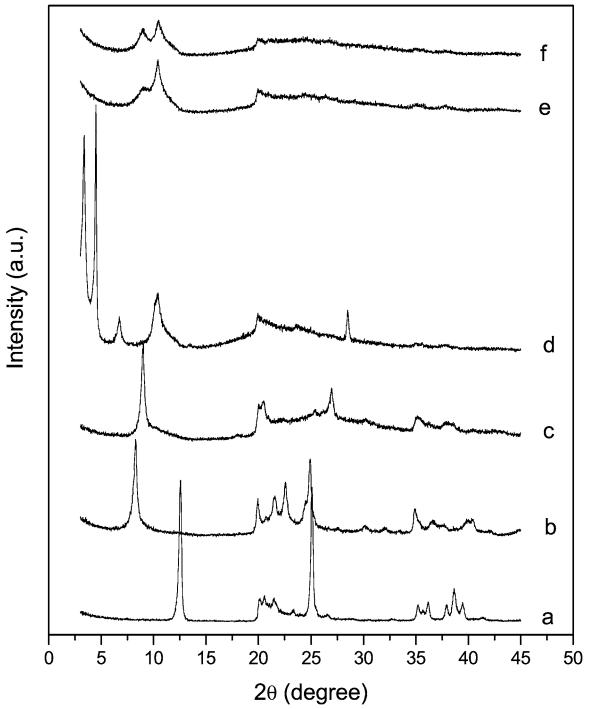

Fig. 3. Powder X-ray diffraction of raw kaolinite (a), kaolinite intercalated with urea (b), kaolinite intercalated with water and still moist (c), **KUH**—still moist (d), **KUH-FP-1** (e) and **KUH-FP-2** (f).

tercalation of the *n*-hexylamine in kaolinite in a double-layer arrangement [25]. **KUH-FP-1** exhibited two peaks near 10° (2θ) with basal distances of 9.78 and 8.60 Å, respectively. The first basal distance of 9.78 Å was attributed to fully hydrated kaolinite; the second, to hydrated kaolinite. According to our proposed mechanism, the presence of water is essential to layer curling, with the diffraction peaks similar to those of layered hydrated kaolinite. In the case of grafted kaolinite, the organic molecules seem to play an important role in the curling process, leading to single-walled nanotubes [16].

KUH-FP-2 exhibited two diffraction peaks near 10° (2θ), with basal distances of 9.86 and 8.45 Å, with the same interpretation as for **KUH-FP-1**. The small differences between the values can be related to the experimental error or an influence of the different porphyrin. It is important to emphasize that the presence of interstratified phases, where random mixtures of phases are present, are characterized by the broad diffraction peaks in the final phases.

Analysis of the supernatant of the immobilization of the iron porphyrins was performed by UV–vis spectroscopy (not shown). Using the Lambert–Beer law, the percentages of immobilization were calculated; the results were 59% for **KUH-FP-1** [Fe(TPFPP) in toluene, 406 nm ($\varepsilon = 89 \times 10^3$ L mol^{-1} cm^{-1})] and 100% for **KUH-FP-2** [Fe(TDFSPP) in water, 390 nm ($\varepsilon = 37 \times 10^3$ L mol^{-1} cm^{-1})].

The formation of kaolinite nanotubes (or scroll-like structures) was confirmed by TEM (Fig. 4), but with the predominance of layered or nonexfoliated kaolinite (Figs. 4c and 4d). This can be attributed to the low power of the ultrasonic bath, because the nanotubes were frequently observed when the procedure was repeated (not shown). The tubes had different outer diameters, and some had a ragged structure (Fig. 4b), attributed to the incomplete curling process. Considering that the raw kaolinite had a crystal size around 0.2/3 μm, it can be supposed that the curling process occurred without breaking the original layers, but by detaching the outer layers of the crystals (small amounts or even single layers) and curling until the crystal layers were totally transformed into rolled-up structures. Actually, in kaolinite the curling process is thermodynamically favorable when the hydrogen bonds of the kaolinite structure are weakened by the intercalation of large molecules like *n*-hexylamine or others. The inner diameter of the tubes was variable, with the smallest around 250 Å. It is possible to trap a single molecule of iron porphyrin with diameters close to one-tenth that size.

We cannot infer much about the position of the iron porphyrin molecules in the solid, but we can exclude intercalation between the layers and assume the presence inside the rolled-up tubes, because the inner diameter is large enough to lodge single iron porphyrin molecules. Because the surface area of the compound is likely high, the presence of a catalytic active site between the crystals and/or tubes is also possible, especially for the charged iron porphyrin, where the interaction with the aluminol surface groups is most likely.

Fig. 5 shows a schematic representation for catalyst intercalation and preparation. Step 1 involves the mechanochemical intercalation of urea, and step 2 involves the intercalation of *n*-hexylamine. Step 3 occurs after the addition of iron porphyrins in the presence of an ultrasonic bath. Step 4 refers to the process of washing the urea-intercalated kaolinite, and step 5 refers to washing the **KUH**. The phases obtained from steps 4 and 5 are also present in step 3, whether curled or not.

The catalytic activities of both iron porphyrins (homogeneous catalysis) and the corresponding supported catalysts, **KUH-FP-1** and **KUH-FP-2** (heterogeneous catalysis), were investigated on the oxidation of two substrates: cyclic (cyclohexane) and linear alkane (*n*-heptane). The results are displayed in Table 1 for cyclohexane and *n*-heptane products. The oxidation of cyclohexane with iodosylbenzene in the presence of metalloporphyrins was generally found to yield cyclohexanol and cyclohexanone as major products as a biomimetic cytochrome P-450 model. High selectivity for the alcohol product was also observed.

Table 1 shows that both iron porphyrins exhibited catalytic activity for the oxidation of cyclohexane (homogeneous catalysis). Both iron porphyrins studied here would be expected to exhibit high efficiency for oxidation, because they are robust and efficient porphyrin structures due to the presence of electronegative substituents on the phenyl ring, which contribute to reducing the electronic density on the porphyrin ring, stabilizing it against oxidative degradation [7]. In fact, high yield (69%) and high selectivity for cyclohexanol were observed for the Fe(TPFPP). The opposite behavior was observed for the charged porphyrin Fe(TDFSPP), which can be attributed to the poor solubility of this complex in the solvent mixture used for the catalytic reactions. The insolubility problems were minimized when the anionic iron porphyrin was immobilized on kaolinite (**KUH-FP-2**). In this situation, the efficiency was im-

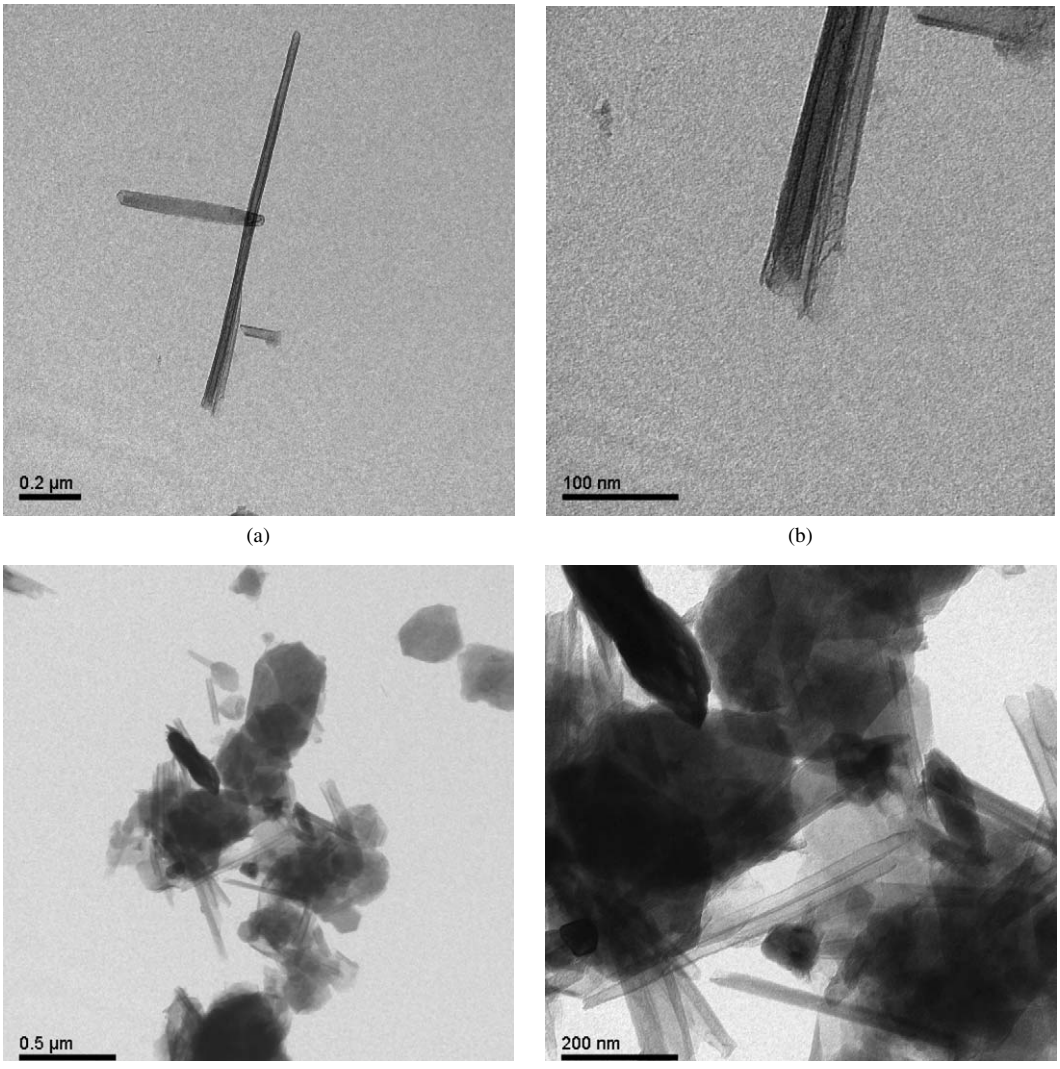

Fig. 4. Transmission electron micrographs of **KUH-FP-2**.

proved, and only alcohol was produced using **KUH-FP-2** (heterogeneous catalysis).

Different reaction solvents were also tried (acetonitrile [ACN], dichloromethane [DCM], and dichloroethane) to study their influence in the behavior of the catalyst. Interesting results were obtained for the polar iron porphyrin Fe(TDFSPP) and the heterogeneous catalyst **KUH-FP-2**. The results obtained in dichloroethane were also similar to those obtained in dichloromethane (not shown in Table 1).

It can be seen that in the oxidation of cyclohexane in homogeneous catalysis, the solubility of the catalyst is an important factor, with the best results obtained in acetonitrile (where the solubility of the polar iron porphyrin is higher) compared with pure DCM or a DCM–ACN mixture. On the other hand, for the heterogeneous catalysis, the best results were obtained in the DCM–ACN mixture. In this case, the results suggest that the access of the oxidant iodosylbenzene and the substrate to the immobilized active site are the most important factors. When heptane was used as a substrate, similar results were also observed, but it is interesting to note that in pure dichloromethane, where both substrates are soluble, the lower yields were always produced. In this condition, the presence of ketone can suggest that when the alcohol was produced, the solvent with low polarity was not efficient in removing it away from the surrounding catalytic site, and the oxidation proceeded to ketone.

The strong interaction that probably occurs between the charged iron porphyrin [Fe(TDFSPP)] and the kaolinite support (layered crystals or tubes) probably keeps the catalyst on the solid during the catalytic reaction; consequently, no iron porphyrin traces were detected after all of the catalytic reactions using **KUH-FP-2**. This behavior creates the opportunity to reuse the catalysts.

On the other hand, immobilization of the neutral Fe(TPFPP) on the kaolinite (**KUH-FP-1**) mostly deactivated the catalyst, and only 8% of alcohol was observed. Because no iron porphyrin trace was observed after any of the catalytic reactions using **KUH-FP-1,** similar to what was observed with **KUH-FP-2,** it is reasonable to suppose that there is also a strong interaction between the neutral complex and the support. The very low yields observed suggest that the catalytic site is in-

Table 1
Oxidation of cyclohexane and heptane catalyzed by iron porphyrins and immobilized iron porphyrins

Catalyst	Solvent	Cyclohexane oxidation[a]		Heptane oxidation[a]						
		Alcohol yield[b] (%)	Ketone yield[b] (%)	Alcohol yield[b] (%)	Ketone yield[b,c] (%)	Total yield[b] (%)	Alcohol ketone ratio[a]	Regioselectivity[d] (%)			
								C-2		C-3	
								ol	one	ol	one
KUH-FP-1	ACN–DCM	8.0	–	0	0	0	–	–	–	–	–
[Fe(TPFPP)]	ACN–DCM	69	5.0	46	11.5	69	4	61	82.6	39	17.4
KUH-FP-2	ACN–DCM	28	–	71	4.0	79	18	60.6	–	39.4	100
	DCM	14	–	–	9.0	18	0	–	–	–	100
	ACN	21	–	55	5.0	65	11	100	–	–	100
[Fe(TDFSPP)]	ACN–DCM	19	7.0	31	6.0	43	5.2	100	–	–	100
	DCM	9.0	2.0	–	7.0	14	0	–	–	–	100
	ACN	33	Trace	33	3.0	39	11	100	–	–	100
Raw kaolinite		Trace	Trace	–	–	–	–	–	–	–	–

[a] Conditions: catalyst:oxidant:cyclohexane molar ratio = 1:20:2000; solvent mixture acetonitrile/dichloromethane, ACN–DCM (1:1, v/v) or dichloromethane (DCM) or acetonitrile (ACN) at room temperature under argon. Homogeneous catalyses were made under identical conditions as heterogeneous catalyses.
[b] Yield based on starting PhIO (it was assumed that 2 mol of iodosylbenzene were used for the ketone formation).
[c] C-2 and C-3 heptane products of oxidation (alcohol and ketone); it was not observed yield for products correspondent for the C-1 and C-4 heptane positions.
[d] Relative proportions of products (%) at positions C-2 and C-3 of heptane. The positions C-1 and C-4 of heptane did not presented product yields. ol = heptanol and one = heptanone.

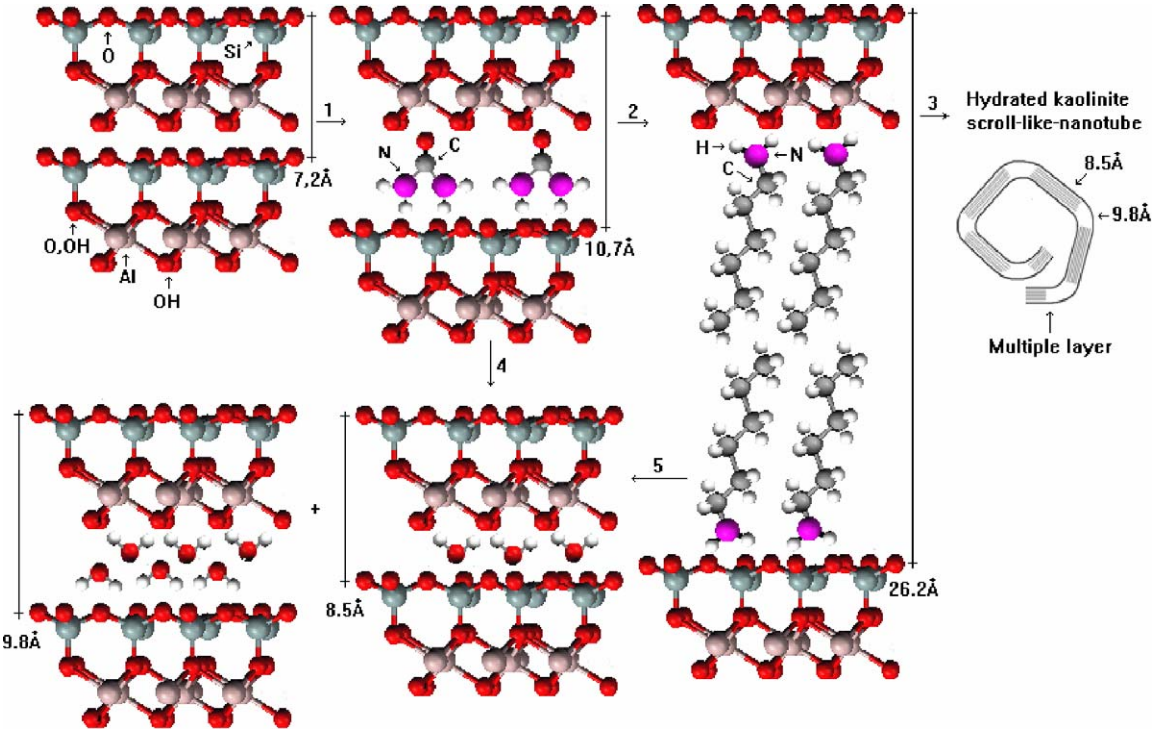

Fig. 5. Schematic representation of the steps followed during the preparation of the catalyst.

accessible to the substrate and oxidant. This could occur because the iron porphyrin is firmly attached inside the tubes or in layered kaolinite crystal agglomerates. The site could even be located in single-layer agglomerates with a "castle of cards" morphology, resulting from the exfoliation process. Another possibility could be that both the fifth and sixth coordinative positions of the iron are blocked by the bond of ligands from the support, preventing interaction with the oxidant iodosylbenzene and, consequently, the catalytic active species [26,27]. Yet another possibility is coordination of the iron porphyrin with hexylamine/urea, which can deactivate the catalyst.

Frequently, metalloporphyrins or other complexes, transition metal ions either in solution or immobilized, are used for oxidation of linear alkanes such as *n*-heptane [15,27–31]. The regioselectivity in the oxidation process using metalloporphyrins and in the absence of steric restraints is essentially under thermodynamic control [32]. The product distribution observed is consistent with formation of a radical intermediate species produced

by hydrogen atom abstraction [33]. Consequently, the rate of the products observed is related to the C–H bond strength, with more products expected from oxidation at tertiary and secondary carbon than from oxidation at primary carbon [29].

On the other hand, in the presence of steric constraints, caused by the support when the metalloporphyrin is immobilized [15] or by the porphyrin structure [34], the efficiency and selectivity in the oxidation of linear alkanes can be altered. This behavior was observed with the two iron porphyrins in solution or immobilized in kaolinite.

The yields of heptane oxidation products (Table 1) reflect the same result observed for cyclohexane oxidation: In homogeneous catalysis, Fe(TPFPP) was more efficient than Fe(TDFSPP) for converting the substrate to alcohol at positions 2 and 3 (because quantitative yields below 2% were not observed for products at position C-1 or C-4, as would be expected for oxidation of the linear alkane). A tendency for selectivity toward alcohol instead of ketone was also observed.

For the neutral iron porphyrin, the rate of the products observed is as expected, with more alcohol (61% of the total) and more ketone (2.6% of the total) produced at position C-2 than at position C-3. Instead of the lower efficiency, the charged Fe(TDFSPP) presented high selectivity for the C-2 position of alcohol and the C-3 position of ketone (Table 1, regioselectivity % data).

Normally in metalloporphyrins, there is no discrimination between secondary sites (i.e., C-2 and C-3), with the ratio of yield products at these sites (2-heptanol/3-heptanol yields) close to 1, as observed for the unhindered metallotetraphenylporphyrin [35]. The selectivity observed in the heterogeneous catalysis for the most accessible secondary site (C-2) was higher for Fe(TDFSPP) (31% of 2-heptanol) than for Fe(TPFPP). The presence of the sulphonate groups at the meta position of the meso phenyl groups of the porphyrin rings of Fe(TDFSPP) and the negative charges probably would make it difficult for the substrate to gain access to the metal center, with this iron porphyrin more hindered for the secondary C-3 heptane position. If any 3-heptanol was produced, it was probably converted to 3-heptanone.

After immobilization, the catalytic behavior changed for the two catalyst complexes; for example, for **KUH-FP-1,** no activity was observed in the oxidation of heptane. The catalytic efficiency for the hydroxylation appeared to arise by controlling the access of the substrate to the active oxidant site or the access of iodosylbenzene to generate the oxidant site. The access of the alkane to the metal was restricted by the kaolinite support in the case of the **KUH-FP-1**, because both substrates showed low or zero activity for catalytic oxidation even for the more thermodynamically favorable C-2 and C-3 positions in linear alkanes.

KUH-FP-2, on the other hand, exhibited high yields of alcohol and ketone (total yield, 79%), but in contrast to the iron porphyrin in solution, alcohol at positions C-2 and C-3 was observed with rates similar to those observed for iron porphyrins in general [35]. Because no Fe(TDFSPP) leaching was observed during the heterogeneous catalytic reactions with **KUH-FP-2**, which might justify the drastic catalytic behavior changes observed, it is reasonable to assume that the immobilization of Fe(TDFSPP) occurs through the strong charge interaction between the solid support and the porphyrin ring sulphonate groups. This interaction would expose the catalytic active site, facilitating mainly the access of C-2 and to a lesser extent the secondary site C-3.

In summary, the catalytic results in cyclohexane and heptane oxidation presented here show that the catalytic solid obtained from the interaction of iron porphyrin and kaolinite was directly dependent on the structure of the ring complex. The material resulting from the interaction of the neutral iron porphyrin [Fe(TPFPP)] and the kaolinite generated a catalytic solid that was more inaccessible to the substrate. Another possibility is that the active site was partially inactivated by the coordination of residual hexylamine/urea. On the other hand, the immobilization of the tetra negatively charged Fe(TDFSPP) in kaolinite generated a more efficient catalyst in comparison with the neutral compound and homogeneous catalysis.

Finally, none of the oxidation products from cyclohexane or heptane were found in the absence of iron porphyrins or using just raw kaolinite. This demonstrates that the iron complexes in fact mediated the oxygen atom transfer from the iodosylbenzene to the substrates.

4. Conclusion

The process of intercalating urea between the layers of kaolinite is believed to weaken the interlayer hydrogen bonds, allowing the access of larger molecules and consequently delamination of the layers, which can curl and produce the so called “halloysite-like” morphology [16], tubular or scroll-like kaolinite. This curling process is performed with the aid of an ultrasonic bath. The curled nanotubes and delaminated crystals thus obtained, having high surface areas, can immobilize neutral [Fe(TPFPP)] or anionic-charged [Fe(TDFSPP)] iron porphyrins, which can be used as oxidation catalysts.

The activity differences for catalysts in homogeneous and heterogeneous media can be explained by the different interactions of the metalloporphyrins and kaolinite. In **KUH-FP-1**, the neutral porphyrin was probably inserted in the nanotubes or trapped between the crystals, impairing access of iodosylbenzene and/or the substrate to the catalytically active site. Another possible explanation is deactivation of the catalytic site by hexylamine/urea used in the catalyst preparation. In **KUH-FP-2**, the anionic porphyrin probably interacted with the outer surface of the tubes and/or layers through aluminol bonds.

Acknowledgments

The authors thank the Conselho Nacional de Desenvolvimento Científico e Tecnológico (CNPq), Coordenação de Aperfeiçoamento de Pessoal de Nível Superior (CAPES), Fundação Araucária, Fundação da Universidade Federal do Paraná (FUNPAR), and Universidade Federal do Paraná (UFPR) for the financial support. They also thank the Centro de Microscopia Eletrônica da UFPR for the TEM analyses.

References

[1] M.M. Ramirez-Corredores, Appl. Catal. 197 (2000) 3.
[2] J. Harber, L. Matachowski, K. Pamin, J. Poltowicz, J. Mol. Catal. A Chem. 162 (2000) 105.
[3] J. Harber, L. Matachowski, K. Pamin, J. Poltowicz, J. Mol. Catal. A Chem. 198 (2003) 215.
[4] J.R. Lindsay Smith, Metalloporphyrins in Catalytic Oxidations, Marcel Dekker, New York, 1994, pp. 325–361.
[5] T. Aida, S. Inoue, in: K.M. Kadish, K.M. Smith, R. Guilard (Eds.), The Porphyrin Handbook, Academic Press, San Diego, 1999, pp. 133–156.
[6] B. Meunier, Chem. Rev. 92 (1992) 1411.
[7] D. Dolphin, T.G. Traylor, L.Y. Xie, Acc. Chem. Res. 30 (1997) 251.
[8] D. Mansuy, Coord. Chem. Rev. 125 (1993) 129.
[9] D. Mansuy, Metalloporphyrins in Catalytic Oxidations, Marcel Dekker, New York, 1994, p. 99.
[10] D.C. de Oliveira, H.C. Sacco, O.R. Nascimento, Y. Iamamoto, K.J. Ciuffi, J. Non-Cryst. Solids 284 (2001) 27.
[11] J.E. Gardolinski, P.G. Peralta-Zamora, F. Wypych, J. Colloid Interface Sci. 211 (1999) 137.
[12] J.L. Guimarães, P.G. Peralta-Zamora, F. Wypych, J. Colloid Interface Sci. 206 (1998) 281.
[13] F. Wypych, in: F. Wypych, K.G. Satyanarayana (Eds.), Clay Surfaces, Fundamentals and Applications, Academic Press/Elsevier, 2004.
[14] J.E. Gardolinski, M.P. Cantão, F. Wypych, Quim. Nova 24 (2001) 761.
[15] S. Nakagaki, F.L. Benedito, F. Wypych, J. Mol. Catal. A Chem. 217 (2004) 121.
[16] J.E.F.C. Gardolinski, Ph.D. Thesis, University of Kiel, Germany, 2005.
[17] J.E. Gardolinski, H.P. Martins, F. Wypych, Quim. Nova 26 (2003) 30.
[18] J.G. Sharefkin, H. Saltzmann, Org. Synth. 43 (1963) 62.
[19] J. Lucas, E.R. Kennedy, M.W. Forno, Org. Synth. 43 (1963) 483.
[20] J.S. Lindsey, J. Org. Chem. 54 (1987) 827.
[21] A. Adler, F.R. Longo, J. Am. Chem. Soc. 86 (1964) 3145.
[22] M. Halma, A. Bail, F. Wypych, S. Nakagaki, J. Mol. Catal. A Chem. 243 (2006) 44.
[23] R.L. Frost, E. Makó, J. Kristóf, J.T. Kloprogge, Spectrochim. Acta A 58 (2002) 2849.
[24] I. Shimizu, H. Okabayashi, K. Taga, E. Nishio, C.J. O'Connor, Vib. Spectrosc. 14 (1997) 113.
[25] Y. Komori, Y. Sugahara, K. Kuroda, Appl. Clay Sci. 15 (1999) 241.
[26] J.T. Groves, Y. Watanabe, J. Am. Chem. Soc. 110 (1988) 8443.
[27] A.A. Guedes, J.R. Lindsay-Smith, O.R. Nascimento, D.F.C. Guedes, M.D. Assis, J. Braz. Chem. Soc. 16 (4) (2005) 835.
[28] W. Nam, Y.M. Goh, Y.J. Lee, M.H. Lim, C. Kim, Inorg. Chem. 38 (1999) 3238.
[29] M.A. Matinez-Lorente, P. Battioni, W. Kleemiss, J.F. Bartoli, D. Mansuy, J. Mol. Catal. A Chem. 113 (1996) 343.
[30] J.M. Thomas, R. Raja, G. Sankar, R.G. Bell, Acc. Chem. Res. 34 (2001) 191.
[31] K.S. Suslick, P. Bhyrappa, J.-H. Chou, M.E. Kosal, S. Nakagaki, D.W. Smithenry, S.R. Wilson, Acc. Chem. Res. 38 (2005) 283.
[32] K.S. Suslick, S. Van Deusen-Jeffries, in: J.-M. Lehn (Ed.), Comprehensive Supramolecular Chemistry, Elsevier Science, Oxford, 1996, chap. 5.
[33] J.T. Groves, W.J. Kruper, R.C. Haushalter, J. Am. Chem. Soc. 102 (1980) 6375.
[34] K. Suslick, B. Cook, M. Fox, J. Chem. Soc. Chem. Commun. (1980) 580.
[35] C.A. Tolman, J.D. Druliner, M.J. Nappa, N. Herron, in: C.L. Hill (Ed.), Activation and Functionalization of Alkanes, Wiley, New York, 1989, p. 303, chap. 10.